

DMD#20776

Novel Binding Mode of the Acidic CYP2D6 Substrates Pactimibe and its Metabolite,

R-125528

Masakatsu Kotsuma, Hiroyuki Hanzawa, Yoriko Iwata, Kenji Takahashi, and Taro Tokui

Drug Metabolism and Pharmacokinetics Research Laboratories, Daiichi-Sankyo Co., Ltd.,

Tokyo, Japan (M.K., T.T.), Advanced Technology Research Laboratories, Daiichi-Sankyo Co.,

Ltd., Tokyo, Japan (H.H., Y.I.), and Research Laboratories, Kyoto Pharmaceutical Industries,

Ltd., Kyoto, Japan (K.T.)

DMD#20776

Running title: Novel CYP2D6 binding mode of acidic substrates

Corresponding Author: Masakatsu Kotsuma

Address:

DAIICHISANKYO CO., LTD.

1-2-58, Hiromachi, Shinagawa-ku, Tokyo 140-8710, Japan

Phone: +81-2-3492-3131, Fax: +81-3-5436-8567

E-mail: kotsuma.masakatsu.gu@daiichisankyo.co.jp

Text Pages: 39

Abstract: 247 words

Introduction: 695 words

Discussion: 1226 words

Tables: 2

Figures: 3

References: 38

Abbreviations: P450, cytochrome P450; M-2, ω -1 oxidized form of R-125528; LC/MS, liquid chromatography/ mass spectrometry; IFD, induced fit docking

DMD#20776

Abstract

Typical CYP2D6 substrates generally contain a basic nitrogen atom which interacts with Asp³⁰¹ and/or Glu²¹⁶ and an aromatic moiety adjacent to the site of metabolism. Recently, we found novel acidic substrates for CYP2D6, pactimibe and its indole metabolite, R-125528, which are not protonated but are negatively charged at physiological pH. The Km value of R-125528 in CYP2D6 expressing microsomes was determined to be 1.74 μ M, which was comparable to those of typical basic CYP2D6 substrates (1-10 μ M). Pactimibe has lower affinity than R-125528, however, the Km value was comparable to that of metoprolol. Interestingly, their sites of metabolism, the ω -1 position of the N-octyl indoline/indole group, were relatively distant from the aromatic moiety. Pactimibe analogue with an N-decyl chain was similarly labile against CYP2D6, however, analogues with N-hexyl or N-dodecyl chains were stable to CYP2D6. An induced fit docking of the ligands with an X-ray crystal structure of substrate-free CYP2D6 (pdb code 2F9Q) indicated the involvement of an electrostatic interaction between the carboxyl group and Arg²²¹, and hydrophobic interaction between the aromatic moiety and Phe⁴⁸³. The docking model correctly positioned the site of metabolism above the heme. The effect of the N-alkyl chain length of pactimibe analogues on their

DMD#20776

CYP2D6 metabolic stability was plausibly explained by the docking model. In conclusion, we report herein a novel CYP2D6 binding mode for the acidic substrates pactimibe and R-125528. Further investigation, such as a site directed mutation, will be necessary to directly demonstrate the involvement of Arg²²¹ in CYP2D6 binding.

DMD#20776

Introduction

Cytochrome P450 (P450) is a large superfamily of heme containing monooxygenases involved in the oxidation of a wide variety of organic chemicals (Guengerich, 2001). CYP2D6 is one of the best known P450 isoforms and leads to large inter-individual variations in drug concentration, drug response, therapeutic outcome and/or toxicity due to its polymorphic nature (Brynne et al., 1998; Molden et al., 2002; Fux et al., 2005). Although CYP2D6 is a minor component (~2%) of the total P450 content in the human liver, many drugs currently in clinical use are metabolized by CYP2D6, such as antiarrhythmics, antidepressants, antipsychotics, β -blockers, and analgesics (Jones et al., 1997). The variability in CYP2D6 activity is mainly genetically determined, and 5% to 10% of Caucasians are reported to express a poor CYP2D6-metabolizing phenotype, resulting from the inheritance of two mutant null alleles (van der Weide and Steijns, 1999). To reduce the clinical failures derived from polymorphic inter-individual variations in drug response is very important. Therefore, several efforts have been directed to predicting the binding affinity against CYP2D6 (Strobl et al., 1993; de Groot et al., 1999a; de Groot et al., 1999b; Ekins et al., 2003).

DMD#20776

CYP2D6 substrates generally exhibit basic nitrogens that have been predicted to interact with one of two acidic amino acid side-chains, Asp³⁰¹ or Glu²¹⁶, of the enzyme. In early models of CYP2D6, a characteristic common to the vast majority of CYP2D6 substrates is the presence of at least one basic nitrogen atom. Pharmacophore models suggest that the site of oxidation is located about 5 to 7 Å away from the basic nitrogen (Koymans et al., 1992). Ellis *et al.* (1995) demonstrated that Asp³⁰¹ plays an important role in determining the substrate specificity and activity of CYP2D6 and provided experimental evidence for electrostatic interaction between the basic nitrogen in CYP2D6 substrates and the carboxylate group of Asp³⁰¹. Guengerich *et al.* (2003) and Paine *et al.* (2003) suggested the importance of Glu²¹⁶ in addition to Asp³⁰¹ as key determinant factors for the substrate specificity and product regioselectivity in CYP2D6.

Another chemical structural property of typical CYP2D6 substrate is a flat aromatic moiety near the site of oxidation. Two aromatic phenylalanines, Phe¹²⁰ and Phe⁴⁸³, and several hydrophobic residues such as Leu²¹³ and Val³⁰⁸ (Keizers et al., 2004; Flanagan et al., 2004; de Graaf et al., 2007) have been proposed as active site residues. The hydrophobic pocket defined by these hydrophobic residues is thought to interact with the hydrophobic regions in

DMD#20776

the substrate.

However, Guengerich *et al.* (2002) identified a CYP2D6 substrate, spiro-sulfonamide, devoid of basic nitrogen, raising a question about the current CYP2D6 model based on a critical electrostatic interaction. Due to the absence of a basic nitrogen atom in its structure, no hydrogen bonds are formed to the negatively charged residues, Asp³⁰¹ and/or Glu²¹⁶. Thereafter, Kemp *et al.* (2004) docked spiro-sulfonamide positioned between the two phenylalanine residues, Phe¹²⁰ and Phe⁴⁸³ in a CYP2D6 homology model.

Recently, we found novel substrates for CYP2D6, pactimibe sulfate and its indole metabolite, R-125528, which are acidic compounds with a carboxyl group and no basic nitrogen in their structures (Kotsuma *et al.*, 2008b). In human clinical drug-drug interaction study, the AUC_{0-72h} of pactimibe and R-125528 were increased 1.7- and 5.0-fold by cotreatment of quinidine, respectively (Kotsuma *et al.*, 2008a). Interestingly, their sites of metabolism are relatively far from the aromatic moiety (Figure 1B, the ω -1 position of the N-octyl chain), where oxidation often occurs in typical CYP2D6 substrates. Pactimibe sulfate (formerly named CS-505, Figure 1A), which was discovered by Kyoto Pharmaceutical Industry, is a novel water soluble antioxidative acyl coenzyme A:cholesterol acyltransferase

DMD#20776

inhibitor for the treatment of hypercholesterolemia and atherosclerotic diseases (Kamiya et al., 1997; Kamiya et al., 2000; Kitayama et al., 2006a; Kitayama et al., 2006b; Kitayama et al., 2006c; Nissen et al., 2006).

We describe herein the physicochemical properties and CYP2D6 affinity of the novel acidic substrates pactimibe and R-125528. In addition, the CYP2D6 metabolic stability of pactimibe analogues was examined. Very recently, the X-ray crystal structure of substrate-free CYP2D6 was resolved at a resolution of 3.0Å (pdb code 2F9Q) (Rowland et al., 2006). To obtain the possible CYP2D6 binding mode, pactimibe, R-125528, and their structural analogues were docked to substrate free CYP2D6.

DMD#20776

Materials and Methods

Test substances and reagents

Pactimibe sulfate
[7-(2,2-dimethylpropanamido)-4,6-dimethyl-1-octylindoline-5-yl]acetic acid hemisulfate
and R-125528 were synthesized at the Process Development Laboratories, Sankyo Co., Ltd. (Tokyo, Japan). M-2 (ω -1 oxidized form of R-125528) was synthesized at Chemtec Labo., Inc. (Tokyo, Japan). The chemical structure of pactimibe sulfate is shown in Figure 1A. KV-2908, KV-2909, and KV-2915 were synthesized at Kyoto Pharmaceutical Industries, Ltd. Propafenone hydrochloride, desipramine hydrochloride, propranolol hydrochloride, amitriptyline hydrochloride, imipramine hydrochloride, dextromethorphan hydrobromide monohydrate, NADP, glucose-6-phosphate and glucose-6-phosphate dehydrogenase were purchased from Sigma-Aldrich (St. Louis, MO). $MgCl_2 \cdot 6H_2O$ was purchased from Wako Pure Chemical Industries, Ltd (Osaka, Japan). Acetonitrile of high performance liquid chromatography grade and 1N HCl of volumetric analysis grade were purchased from Wako Pure Chemical Industries, Ltd (Osaka, Japan). Other reagents and solvents were of analytical grade and were used without further purification.

DMD#20776

Microsomes expressing human P450 isoforms

CYP2D6*1 + P450 reductase SUPERSOMESTM and Insect Cell Control SUPERSOMESTM prepared from baculovirus infected insect cells were purchased from Gentest (Woburn, MA, USA). The control microsome was used as a control for the native activities. Microsomes were stored at -80°C until use.

Determination of Km values for CYP2D6

All microsomal incubations were carried out at 37°C using 100 mM potassium phosphate buffer (pH 7.4) and an NADPH generating system containing final concentrations of 1.25 mM NADP, 1 mM MgCl₂·6H₂O, 12.5 mM glucose-6-phosphate, and 0.5U/mL glucose-6-phosphate dehydrogenase.

Due to the absence of authentic samples for the metabolites of imipramine, desipramine, amitriptyline, propranolol, dextromethorphan, and propafenone, the substrate depletion method (Obach and Reed-Hagen, 2002) was used for determination of the Michaelis constant (Km) values for typical CYP2D6 substrates. The final CYP2D6 protein concentration and

DMD#20776

substrate concentrations were set at 10 pmol/mL and 0.1, 0.3, 1, 3, 10, and 30 μ M, respectively. Thirty μ L of incubation mixture was added to 90 μ L of ice-cold methanol containing 0.5 μ M of d6-pactimibe as an internal standard at 0, 3, 6, and 9 min to stop the reaction. The mixture was centrifuged at 2,000 rpm for 10 min at 4°C (himac CF7D2, rotor No.: RT3S3-A808, Hitachi Koki, Ltd., Tokyo, Japan). Ten microliters of the supernatant fraction was injected into the liquid chromatography/ mass spectrometry (LC/MS) system for analysis.

For the determination of the K_m value of R-125528, the formation of M-2 was determined. The final CYP2D6 protein concentration and substrate concentrations were set at 10 pmol/mL and 0.3, 1, 3, 10, 30 and 100 μ M, respectively. Under the conditions used, the formation of M-2 was linear with respect to the incubation time and protein concentrations. To stop the reaction, 60 μ L of incubation mixture was added to 120 μ L of ice-cold solution A (acetonitrile/1N hydrochloride/2 mM dithiothreitol; 98:1:1. v/v/v) containing 0.5 μ M of d6-pactimibe as an internal standard and 60 μ L of solution A at 7.5 and 15 min. The mixture was centrifuged at 2,000 rpm for 10 min at 4°C (himac CF7D2, rotor No.: RT3S3-A808, Hitachi Koki, Ltd., Tokyo, Japan). Ten microiliters of the supernatant fraction was injected

DMD#20776

into the LC/MS system for analysis.

Metabolic stability of pactimibe analogues in CYP2D6 expressing microsomes

Microsomal incubations were carried out at 37°C using 100 mM potassium phosphate buffer (pH 7.4) and an NADPH generating system containing final concentrations of 2.5 mM NADP, 10 mM MgCl₂·6H₂O, 25 mM glucose-6-phosphate, and 1U/mL glucose-6-phosphate dehydrogenase. The final CYP2D6 protein concentration was set at 40 pmol/mL. The final concentrations of pactimibe, R-125528, KV-2908, KV-2909, and KV-2915 were set at 1 μM. To stop the reaction, 100 μL of incubation mixture was added to 200 μL of ice-cold solution A containing 0.5 μM of d6-pactimibe as an internal standard at 0, 10, 20 and 30 min. The mixture was centrifuged at 2,000 rpm for 10 min at 4°C (himac CF7D2, rotor No.: RT3S3-A808, Hitachi Koki, Ltd., Tokyo, Japan). Ten microliters of the supernatant fraction was injected into the LC/MS system for analysis.

Determination of pKa

The pKa values for pactimibe and R-125528 were determined using a Sirius GLpKa

DMD#20776

meter.

LC/MS analysis

An LC/MS method was applied for determination of the target analyte. A Waters Alliance 2795 HPLC system (Waters Corporation, Milford, USA) coupled to a Quattro LC (Micromass UK Ltd., Manchester, UK) was used for the detection. The following ions (m/z) were monitored: 267 for desipramine, 278 for amitriptyline, 342 for propafenone, 260 for propranolol, 272 for dextromethorphan, 281 for imipramine, 417.1 for pactimibe, 415.1 for R-125528, 389 for KV-2908, 445 for KV-2909, 473 for KV-2915, and 431.4 for M-2.

Docking methodology

The molecular docking of bufuralol, pactimibe, R-125528, KV-2908, KV-2909, and KV-2915 to CYP2D6 was performed using the crystal structure of substrate free CYP2D6 (pdb code 2F9Q) (Rowland et al., 2006). The substrates were prepared using the LigPrep module of a Maestro (Schrödinger, LLC, New York, NY, 2005). Starting with 2D structures, LigPrep produces a 3D structure with ionization states at pH 7. In the case of pactimibe

DMD#20776

analogues, the carboxyl group carried a formal charge of -1. Induced fit docking (IFD) was carried out using the Prime and Glide module (Sherman et al., 2006) with the default parameter set. In the IFD protocol, the side-chain degrees of freedom in the protein are sampled while allowing small backbone conformational changes through minimization. Docking is carried out using rotamer libraries to sample energetically reasonable side-chains and to eliminate conformations with steric clashes. The docked protein-substrate complexes are ranked according to the IFD score. The IFD score is a composite score made up of the protein/ligand interaction energy (GlideScore) and the protein molecular mechanics energy (Prime energy) in an implicit solvation model (Sherman et al., 2006).

Data analysis

In the substrate depletion experiments (Obach and Reed-Hagen, 2002), the analyte/internal standard peak area ratios were determined and normalized to the value obtained at $t=0$. The percentage remaining versus the time at each substrate concentration was fitted to first order decay functions to determine the initial substrate depletion rate constants (k_{dep}). If the substrate decline demonstrated nonlinearity on the log percentage remaining

DMD#20776

versus time curves, only those initial time points wherein log-linearity was observed were used to determine the depletion rate constants. The K_m values from the substrate consumption experiments were determined by plotting the k_{dep} versus the substrate concentration on a linear-log plot using the following equation:

$$k_{dep} = k_{dep([S] = 0)} \times \left(1 - \frac{[S]}{[S] + K_m} \right)$$

where $[S]$ and $k_{dep([S]=0)}$ represent the substrate concentration and the theoretical maximum consumption rate constant at an infinitesimally low-substrate concentration, respectively.

The K_m value of R-125528 was calculated by fitting the data to the following equation:

$$V = \frac{V_{max} \times [S]}{K_m + [S]}$$

where V and $[S]$ represent the initial rate of M-2 formation and the concentration of R-125528 in the microsomal incubation mixture, respectively. Data analysis was performed with WinNonlin (Ver 4.0.1, Scientific Consulting Inc., Apex, N.C.) and Microsoft Excel 2003 (SP1, Microsoft Corp., Redwood, WA).

DMD#20776

Results

Molecular weight, pKa, and Km values of pactimibe, R-125528, and typical CYP2D6 substrates

The molecular weight, pKa, and Km values of typical CYP2D6 substrates are listed in Table 1. The molecular weight and pKa values of bufuralol, debrisoquine, imipramine, desipramine, nortriptyline, amitriptyline, propranolol, dextromethorphan, metoprolol, and propafenone are cited from Lewis DFV (2004). The Km values of typical CYP2D6 substrates were determined by the substrate depletion method or were derived from articles. The molecular weight and Km values of the atypical CYP2D6 substrates spiro-sulfonamide, pactimibe and R-125528 are compared with those of typical CYP2D6 substrates.

The pKa values of pactimibe and R-125528 were quite low among those of typical CYP2D6 substrates. As shown in Table 1, the pKa values of typical CYP2D6 substrates are generally higher than 8. On the other hand, pKa₁ (for nitrogen in indoline ring) and pKa₂ (for carboxyl group) of pactimibe were 3.39 and 4.34, respectively. The nitrogen in the indole ring of R-125528 was not protonated over the entire pH range and for the carboxyl group only pKa was determined as 4.45, suggesting that they are not positively charged in a physiological

DMD#20776

condition. Spirosulfonamide has also been reported as a non-positively charged CYP2D6 substrate at neutral pH (Guengerich et al., 2002).

The molecular weights of pactimibe and R-125528 were relatively high compared to those of typical CYP2D6 substrates. Those of almost typical CYP2D6 substrates are ranged from 200 to 300. On the other hand, those of pactimibe and R-125528 were 416.6 and 414.6, respectively.

Interestingly, however, pactimibe and R-125528 showed relatively high affinity for CYP2D6. The K_m values of pactimibe and R-125528 for CYP2D6 were determined to be 25.1 and 1.74 μM , respectively. These values were comparable to those of typical CYP2D6 substrates. The K_m values of bufuralol, debrisoquine, imipramine, desipramine, nortriptyline, amitriptyline, propranolol, dextromethorphan, metoprolol, and propafenone, were 3.4 (Emoto et al., 2006), 73.7 (Shen et al., 2007), 2.68, 1.26, 2.08 (Venkatakrisnan et al., 1999), 1.61, 1.48, 0.58, 21.6 (Uttamsingh et al., 2005) and 0.01 μM , respectively.

CYP2D6 metabolic stability of pactimibe analogues

We examined the effect of the N-alkyl chain length of pactimibe analogues on their

DMD#20776

metabolic stability against CYP2D6. The chemical structures of pactimibe analogues and their metabolic stability in CYP2D6 expressing microsomes are shown in Table 2. After 30 min incubation in CYP2D6 expressing microsomes, the metabolic stability (% of 0 min) of pactimibe (C8), R-125528 (C8), KV-2908 (C6), KV-2909 (C10), and KV-2915 (C12) was determined to be 27.5, 0.8, 97.0, 38.1, and 98.4, respectively. While substitution of the N-octyl chain to the N-decyl chain did not change the stability against CYP2D6, the N-hexyl or N-dodecyl chain improved the CYP2D6 metabolic stability.

CYP2D6 docking of pactimibe analogues

At first, we docked a typical CYP2D6 substrate, bufuralol, into the crystal structure of substrate-free CYP2D6 (pdb code 2F9Q) (Rowland et al., 2006) using the induced fit docking mode of the Prime and Glide module for a feasibility assessment. Electrostatic interaction between basic nitrogen and Glu²¹⁶ was observed (Figure 2A). In addition, the aromatic moiety of bufuralol was located in the hydrophobic region defined by hydrophobic residues such as Phe¹²⁰, Phe⁴⁸³, Leu²¹³ and Val³⁰⁸ etc. The docking model correctly identified the reported site of the metabolism of bufuralol (de Groot et al., 1999a; de Graaf et al., 2007).

DMD#20776

To discover the possible docking mode of pactimibe analogues against CYP2D6, we also docked them into the crystal structure of CYP2D6. By an induced fit docking procedure, we generally obtained 5 to 12 poses and the IFD scores ranged from 1.8 to 4.1 kcal/mol. Among them, we considered the structure with the alkyl chain the closest to heme to be representative. In practice, the top or second ranked pose could be selected as the representative structure for each compound and these structures were used for further analysis.

The docking model of R-125528 is shown in Figure 2B. The docking positioned the indole ring of R-125528 close to Phe⁴⁸³ by hydrophobic interaction. In addition, the docking indicated electrostatic interaction between the carboxyl group of R-125528 and the basic residues of Arg²²¹. Interestingly, in contrast to bufurarol docking, the aromatic moiety was not located close to the heme. Instead, an N-octyl chain was inserted into the active site, exhibiting interactions between hydrophobic residues, such as Phe¹²⁰, Leu²¹³, and Leu⁴⁸⁴ etc. Hence, the docking correctly positioned the site of the metabolism of R-125528 at the ω -1 position of the N-octyl chain (Kotsuma et al., 2008b), above the heme. The distance between the ω -1 position of the N-octyl chain and the heme was 4.4Å.

DMD#20776

The docking models of pactimibe (C8), KV-2908 (C6), KV-2909 (C10), and KV-2915 (C12) are shown in Figure 3. When pactimibe and KV-2909 (C10) were docked to CYP2D6, hydrophobic interaction between Phe⁴⁸³ and the indoline ring and electrostatic interaction between the carboxyl group and the basic residues of Arg²²¹ were indicated (Figure 3A and C). The N-alkyl chain was inserted into the hydrophobic region defined by hydrophobic residues such as Leu²¹³, Met³⁷⁴, and Leu⁴⁸⁴ etc. The ω -1 position of the N-alkyl chain was located above the heme and the distances between the ω -1 position of N-octyl chain and N-decyl chain and the heme were 5.0Å and 5.3Å, respectively. On the other hand, when KV-2908 (C6) and KV-2915 (C12) were docked, a different binding mode was suggested. The distance between the ω -1 position of the N-hexyl chain and the heme was 4.3Å. However, no hydrophobic interaction between the indoline ring of KV-2908 and Phe⁴⁸³ was observed (Figure 3B). Regarding the docking model of KV-2915, the direction of the N-dodecyl chain was not towards the heme but towards the entrance of the enzyme (Figure 3D).

DMD#20776

Discussion

Pactimibe and R-125528 were demonstrated to be good substrates for CYP2D6. The K_m value of R-125528 was determined to be 1.74 μM , which was comparable to those of typical CYP2D6 substrates (1-10 μM) (Table 1). Pactimibe has lower affinity than R-125528, however, the K_m value was still comparable to that of metoprolol.

Pactimibe and R-125528 are novel acidic ligands for CYP2D6 in contrast to the vast majority of typical CYP2D6 substrates, which contain basic nitrogen in their structures. It has been suggested that an electrostatic interaction between a protonated basic nitrogen and a carboxyl group of Glu²¹⁶ and/or Asp³⁰¹ plays an important role in determining substrate specificity. As shown in Table 1, the pKa values of typical CYP2D6 substrates are generally more than 8, suggesting that the basic nitrogens are protonated at physiologically equivalent pH. However, the pKa value for a nitrogen in the indoline ring of pactimibe is 3.39. Moreover, nitrogen in the indole ring of R-125528 is not protonated over the entire pH range. Considering that pactimibe and R-125528 possess a carboxylic acid in their structures, they are negatively charged in a physiological condition.

As far as we know, pactimibe and R-125528 are the first identified acidic ligands for

DMD#20776

CYP2D6 with a carboxyl group in their structures, even though there were several reports of non-basic ligands for CYP2D6. Guengerich *et al.* (2002) identified a high affinity ligand, spiro-sulfonamide, devoid of basic nitrogen. It has also been reported that peptide-mimetic compounds having no basic nitrogen (Kumar *et al.*, 1996) and some steroids (Niwa *et al.*, 1998) are CYP2D6 substrates. These findings suggest that the presence of basic nitrogen is not a common requirement for high-affinity CYP2D6 substrates.

To obtain a possible docking mode of acidic ligands against CYP2D6, we conducted an induced fit docking of the ligands with an X-ray crystal structure of substrate-free CYP2D6 (pdb code 2F9Q) recently reported by Rowland *et al.* (2006). At first, we tested a typical CYP2D6 substrate, bufuralol, (Figure 2A) for a feasibility assessment. The docking mode of bufuralol showed a typical CYP2D6 binding mode, indicating electrostatic interaction between a basic nitrogen of bufuralol and Glu²¹⁶. The aromatic ring and its accompanying short alkyl chain, where the metabolism reaction occurs (de Graaf *et al.*, 2007), were correctly located above the heme surrounded by a hydrophobic region defined by Phe¹²⁰, Phe⁴⁸³, Leu²¹³ and Val³⁰⁸. This observation coincided with the general finding that aromatic moieties of CYP2D6 substrates are located between Phe¹²⁰ and several hydrophobic residues such as

DMD#20776

Leu²¹³ and Val³⁰⁸ (de Graaf et al., 2007) and are further metabolized.

In contrast, pactimibe and R-125528 showed a novel binding mode (Figures 2B, 3A).

The aromatic indoline/indole ring was sequestered from the heme by electrostatic interaction with Arg²²¹ and hydrophobic interaction with Phe⁴⁸³, which are located in the access channel.

Instead, the sites of metabolism (ω -1 position of the N-octyl chain), which are relatively distant from the aromatic ring, were located close to the heme. Curiously, the basic residue of Arg²²¹ was proposed to form a salt bridge with the carboxyl group of pactimibe/R-125528.

This result is interesting because it has been generally suggested that electrostatic interaction between the basic nitrogen of a substrate and Glu²¹⁶/Asp³⁰¹ is important for the binding of CYP2D6 substrates (Guengerich et al., 2003; Paine et al., 2003). Further studies, such as a site directed mutation, will be necessary to investigate the involvement of Arg²²¹ in CYP2D6 binding.

Phe⁴⁸³ seems to not only interact with the indoline/indole ring by hydrophobic interaction but also to sterically hinder the access of the main body to the active site. This might be one of the reasons why pactimibe and R-125528 are good ligands for CYP2D6 in spite of their relatively high molecular weight (>400) compared to the other CYP2D6

DMD#20776

substrates (Table 1). In our docking model, while the N-octyl chain was inserted into the active site, the bulky t-butyl and acetic acid moiety was positioned at the entrance of the enzyme. In fact, Smith et al. (1998) pointed out that the bulky phenyl-ring of Phe⁴⁸³ is positioned across the channel mouth, thus limiting the size of the substrate that can access the active site.

This binding model provided a plausible explanation for the difference in the CYP2D6 metabolic stability of pactimibe analogues with N-alkyl chains of different lengths. As shown in Table 2, the metabolic stability of pactimibe (C8) against CYP2D6 was low and was followed by KV-2909 (C10). On the other hand, KV-2908 (C6) was stable against CYP2D6. One possible reason is that the site of metabolism is far from the heme. Actually, by induced fit docking (Figure 3B), the ω -1 position of the N-hexyl chain was close to the heme (4.3Å). However, in this docking model, the orientation of the indoline ring was different compared to that of pactimibe. Then, we docked KV-2908 (C6) using a constraint so that the indoline ring and carboxyl moiety of KV-2908 would be positioned where those of pactimibe are located. As a result, a binding mode similar to that of pactimibe was obtained (data not shown). The distance between the ω -1 position of the N-hexyl chain and the heme was 5.6Å,

DMD#20776

which is more distant than that between the ω -1 position of the N-octyl chain and the heme (5.0 Å).

KV-2915 (C12) was also metabolically stable against CYP2D6, probably because the site of metabolism could not be located in the active site. This docking model suggested that the direction of the N-dodecyl chain was not towards the heme but towards the entrance of the enzyme (Figure 3D). The size of the N-dodecyl chain seems to be too bulky to fit itself into the CYP2D6 active site. Even when we docked KV-2915 to the crystal structure, in which the residue at position 374 is valine (the actual residue in wild-type CYP2D6) instead of methionine (which has a larger residue than valine) used in this study, the long N-dodecyl chain was not accommodated in the active site (data not shown). This observation is in accordance with the result of an in vitro metabolic study using wild-type CYP2D6 expression microsomes.

The CYP2D6 affinity of R-125528 (1.74 μ M) was higher than that of pactimibe (25.1 μ M). This might be due to the difference in lipophilicity between pactimibe and R-125528. The oxidative conversion from the indoline ring to the indole ring changes pactimibe (LogP 4.68) into a more lipophilic metabolite, R-125528 (LogP 5.83). The hydrophobic interaction

DMD#20776

between Phe⁴⁸³ and the indole ring is considered to be more significant compared to that between Phe⁴⁸³ and the indoline ring, even though they showed similar binding modes.

To conclude, we report herein a novel CYP2D6 binding mode for atypical acidic substrates, pactimibe and its metabolite, R-125528. Although they are negatively charged in a physiological condition, their affinities for CYP2D6 were comparable to those of typical basic CYP2D6 substrates. The induced fit docking to CYP2D6 (pdb code 2F9Q) indicated the involvement of an electrostatic interaction between the carboxyl group and Arg²²¹, and a hydrophobic interaction between the aromatic moiety and Phe⁴⁸³. This docking model correctly positioned the site of metabolism (the ω -1 position of the N-octyl chain) above the heme. The effect of the N-alkyl chain length of pactimibe analogues on their CYP2D6 metabolic stability was plausibly explained by this molecular docking model. Further studies, such as a site directed mutation, will be necessary to investigate the involvement of Arg²²¹ in CYP2D6 binding.

DMD#20776

References

Brynne N, Dalen P, Alvan G, Bertilsson L and Gabrielsson J (1998) Influence of CYP2D6

polymorphism on the pharmacokinetics and pharmacodynamic of tolterodine. *Clin*

Pharmacol Ther **63**:529-539.

de Graaf C, Oostenbrink C, Keizers PH, van Vugt-Lussenburg BM, van Waterschoot RA,

Tschirret-Guth RA, Commandeur JN and Vermeulen NP (2007) Molecular

modeling-guided site-directed mutagenesis of cytochrome P450 2D6. *Curr Drug*

Metab **8**:59-77.

de Groot MJ, Ackland MJ, Horne VA, Alex AA and Jones BC (1999a) Novel approach to

predicting P450-mediated drug metabolism: development of a combined protein and

pharmacophore model for CYP2D6. *J Med Chem* **42**:1515-1524.

de Groot MJ, Ackland MJ, Horne VA, Alex AA and Jones BC (1999b) A novel approach to

predicting P450 mediated drug metabolism. CYP2D6 catalyzed N-dealkylation

reactions and qualitative metabolite predictions using a combined protein and

pharmacophore model for CYP2D6. *J Med Chem* **42**:4062-4070.

Ekins S, Berbaum J and Harrison RK (2003) Generation and validation of rapid

DMD#20776

computational filters for cyp2d6 and cyp3a4. *Drug Metab Dispos* **31**:1077-1080.

Ellis SW, Hayhurst GP, Smith G, Lightfoot T, Wong MM, Simula AP, Ackland MJ, Sternberg

MJ, Lennard MS, Tucker GT and et al. (1995) Evidence that aspartic acid 301 is a

critical substrate-contact residue in the active site of cytochrome P450 2D6. *J Biol*

Chem **270**:29055-29058.

Emoto C, Murase S and Iwasaki K (2006) Approach to the prediction of the contribution of

major cytochrome P450 enzymes to drug metabolism in the early drug-discovery stage.

Xenobiotica **36**:671-683.

Flanagan JU, Marechal JD, Ward R, Kemp CA, McLaughlin LA, Sutcliffe MJ, Roberts GC,

Paine MJ and Wolf CR (2004) Phe120 contributes to the regiospecificity of

cytochrome P450 2D6: mutation leads to the formation of a novel dextromethorphan

metabolite. *Biochem J* **380**:353-360.

Fux R, Morike K, Prohmer AM, Delabar U, Schwab M, Schaeffeler E, Lorenz G, Gleiter CH,

Eichelbaum M and Kivisto KT (2005) Impact of CYP2D6 genotype on adverse effects

during treatment with metoprolol: a prospective clinical study. *Clin Pharmacol Ther*

78:378-387.

DMD#20776

Guengerich FP (2001) Common and uncommon cytochrome P450 reactions related to metabolism and chemical toxicity. *Chem Res Toxicol* **14**:611-650.

Guengerich FP, Hanna IH, Martin MV and Gillam EM (2003) Role of glutamic acid 216 in cytochrome P450 2D6 substrate binding and catalysis. *Biochemistry* **42**:1245-1253.

Guengerich FP, Miller GP, Hanna IH, Martin MV, Leger S, Black C, Chauret N, Silva JM, Trimble LA, Yergey JA and Nicoll-Griffith DA (2002) Diversity in the oxidation of substrates by cytochrome P450 2D6: lack of an obligatory role of aspartate 301-substrate electrostatic bonding. *Biochemistry* **41**:11025-11034.

Jones BC, Tyman CA and Smith DA (1997) Identification of the cytochrome P450 isoforms involved in the O-demethylation of 4-nitroanisole in human liver microsomes. *Xenobiotica* **27**:1025-1037.

Kamiya S, Shirahase H, Matsui H, Nakamura S and Wada K (1997) Patent PCT Int WO9712860 A1 19970410

Kamiya S, Shirahase H, Matsui H, Nakamura S and Wada K (2000) U.S. patent 6063860

Keizers PH, Lussenburg BM, de Graaf C, Mentink LM, Vermeulen NP and Commandeur JN (2004) Influence of phenylalanine 120 on cytochrome P450 2D6 catalytic selectivity

DMD#20776

and regiospecificity: crucial role in 7-methoxy-4-(aminomethyl)-coumarin metabolism.

Biochem Pharmacol **68**:2263-2271.

Kemp CA, Flanagan JU, van Eldik AJ, Marechal JD, Wolf CR, Roberts GC, Paine MJ and

Sutcliffe MJ (2004) Validation of model of cytochrome P450 2D6: an in silico tool for

predicting metabolism and inhibition. *J Med Chem* **47**:5340-5346.

Kitayama K, Koga T, Inaba T and Fujioka T (2006a) Multiple mechanisms of

hypocholesterolemic action of pactimibe, a novel acyl-coenzyme A:cholesterol

acyltransferase inhibitor. *Eur J Pharmacol* **543**:123-132.

Kitayama K, Koga T, Maeda N, Inaba T and Fujioka T (2006b) Pactimibe stabilizes

atherosclerotic plaque through macrophage acyl-CoA:cholesterol acyltransferase

inhibition in WHHL rabbits. *Eur J Pharmacol* **539**:81-88.

Kitayama K, Tanimoto T, Koga T, Terasaka N, Fujioka T and Inaba T (2006c) Importance of

acyl-coenzyme A:cholesterol acyltransferase 1/2 dual inhibition for

anti-atherosclerotic potency of pactimibe. *Eur J Pharmacol* **540**:121-130.

Kotsuma M, Tokui T, Freudenthaler S and Nishimura K (2008a) Effects of ketoconazole and

quinidine on pharmacokinetics of pactimibe and its plasma metabolite, R-125528, in

DMD#20776

human. *Drug Metab Dispos.* (in press)

Kotsuma M, Tokui T, Ishizuka-Ozeki T, Honda T, Iwabuchi H, Murai T, Ikeda T and Saji H

(2008b) CYP2D6-Mediated metabolism of a novel acyl coenzyme A:cholesterol

acyltransferase inhibitor, pactimibe, and its unique plasma metabolite, R-125528.

Drug Metab Dispos **36**:529-534.

Koymans L, Vermeulen NP, van Acker SA, te Koppele JM, Heykants JJ, Lavrijsen K,

Meuldermans W and Donne-Op den Kelder GM (1992) A predictive model for

substrates of cytochrome P450-debrisoquine (2D6). *Chem Res Toxicol* **5**:211-219.

Kumar GN, Rodrigues AD, Buko AM and Denissen JF (1996) Cytochrome P450-mediated

metabolism of the HIV-1 protease inhibitor ritonavir (ABT-538) in human liver

microsomes. *J Pharmacol Exp Ther* **277**:423-431.

Lewis DF (2004) Quantitative structure-activity relationships (QSARs) for substrates of

human cytochromes P450 CYP2 family enzymes. *Toxicol In Vitro* **18**:89-97.

Molden E, Johansen PW, Boe GH, Bergan S, Christensen H, Rugstad HE, Rootwelt H,

Reubsaet L and Lehne G (2002) Pharmacokinetics of diltiazem and its metabolites in

relation to CYP2D6 genotype. *Clin Pharmacol Ther* **72**:333-342.

DMD#20776

Nissen SE, Tuzcu EM, Brewer HB, Sipahi I, Nicholls SJ, Ganz P, Schoenhagen P, Waters DD,

Pepine CJ, Crowe TD, Davidson MH, Deanfield JE, Wisniewski LM, Hanyok JJ and

Kassalow LM (2006) Effect of ACAT inhibition on the progression of coronary

atherosclerosis. *N Engl J Med* **354**:1253-1263.

Niwa T, Yabusaki Y, Honma K, Matsuo N, Tatsuta K, Ishibashi F and Katagiri M (1998)

Contribution of human hepatic cytochrome P450 isoforms to regioselective

hydroxylation of steroid hormones. *Xenobiotica* **28**:539-547.

Obach RS and Reed-Hagen AE (2002) Measurement of Michaelis constants for cytochrome

P450-mediated biotransformation reactions using a substrate depletion approach. *Drug*

Metab Dispos **30**:831-837.

Paine MJ, McLaughlin LA, Flanagan JU, Kemp CA, Sutcliffe MJ, Roberts GC and Wolf CR

(2003) Residues glutamate 216 and aspartate 301 are key determinants of substrate

specificity and product regioselectivity in cytochrome P450 2D6. *J Biol Chem*

278:4021-4027.

Rowland P, Blaney FE, Smyth MG, Jones JJ, Leydon VR, Oxbrow AK, Lewis CJ, Tennant

MG, Modi S, Eggleston DS, Chenery RJ and Bridges AM (2006) Crystal structure of

DMD#20776

human cytochrome P450 2D6. *J Biol Chem* **281**:7614-7622.

Shen H, He MM, Liu H, Wrighton SA, Wang L, Guo B and Li C (2007) Comparative metabolic capabilities and inhibitory profiles of CYP2D6.1, CYP2D6.10, and CYP2D6.17. *Drug Metab Dispos* **35**:1292-1300.

Sherman W, Day T, Jacobson MP, Friesner RA and Farid R (2006) Novel procedure for modeling ligand/receptor induced fit effects. *J Med Chem* **49**:534-553.

Smith G, Modi S, Pillai I, Lian LY, Sutcliffe MJ, Pritchard MP, Friedberg T, Roberts GC and Wolf CR (1998) Determinants of the substrate specificity of human cytochrome P-450 CYP2D6: design and construction of a mutant with testosterone hydroxylase activity. *Biochem J* **331 (Pt 3)**:783-792.

Strobl GR, von Kruedener S, Stockigt J, Guengerich FP and Wolff T (1993) Development of a pharmacophore for inhibition of human liver cytochrome P-450 2D6: molecular modeling and inhibition studies. *J Med Chem* **36**:1136-1145.

Uttamsingh V, Lu C, Miwa G and Gan LS (2005) Relative contributions of the five major human cytochromes P450, 1A2, 2C9, 2C19, 2D6, and 3A4, to the hepatic metabolism of the proteasome inhibitor bortezomib. *Drug Metab Dispos* **33**:1723-1728.

DMD#20776

van der Weide J and Steijns LS (1999) Cytochrome P450 enzyme system: genetic

polymorphisms and impact on clinical pharmacology. *Ann Clin Biochem* **36** (Pt

6):722-729.

Venkatakrishnan K, von Moltke LL and Greenblatt DJ (1999) Nortriptyline

E-10-hydroxylation in vitro is mediated by human CYP2D6 (high affinity) and

CYP3A4 (low affinity): implications for interactions with enzyme-inducing drugs. *J*

Clin Pharmacol **39**:567-577.

DMD#20776

Figure Legends

Figure 1. Chemical structure of pactimibe sulfate (A) and metabolic positions of pactimibe, R-125528 (Kotsuma et al., 2008b), and bufuralol (de Graaf et al., 2007) (B). The sites of oxidation by CYP2D6 are indicated by arrows (\uparrow) together with the protonated nitrogen atom (+)

Figure 2. (A) The docking model of a typical CYP2D6 substrate, bufuralol, and CYP2D6. The heme moiety and key residues are also shown. Electrostatic interaction between the basic nitrogen of bufuralol and Glu²¹⁶ were indicated. The aromatic moiety was located above the heme. (B) The docking model of R-125528 and CYP2D6. The heme moiety and key residues are also shown. Hydrophobic interaction between Phe⁴⁸³ and the indole ring and electrostatic interaction between the carboxyl group and basic residues of Arg²²¹ were indicated. In addition, interaction between the N-octyl chain and hydrophobic residues such as Phe¹²⁰, Leu²¹³, and Leu⁴⁸⁴ etc. was observed. The distance between the site of metabolism (ω -1 position of the N-octyl chain) and the heme was 4.4Å.

DMD#20776

Figure 3. (A) The docking model of pactimibe (C8), (B) KV-2908 (C6), (C) KV-2909 (C10), and (D) KV-2915 (C12). (A)(C) Hydrophobic interaction between Phe⁴⁸³ and the indoline ring and electrostatic interaction between the carboxyl group and basic residues of Arg²²¹ were indicated. In addition, interaction between the N-octyl/N-decyl chains and hydrophobic residues such as Leu²¹³, Met³⁷⁴, and Leu⁴⁸⁴ etc. was observed. The distances between the ω -1 position of the N-octyl and N-decyl chains and the heme were 5.0 and 5.3 Å, respectively. (B) The distance between the ω -1 position of the N-hexyl chain and the heme was 4.3 Å. However, no hydrophobic interaction between Phe⁴⁸³ and the indoline ring was observed. (D) The N-dodecyl chain was not directed towards the heme but towards the entrance of the enzyme.

DMD#20776

Table 1. Molecular weight, pKa, and Km values of pactimibe and R-125528 compared with typical CYP2D6 substrates

Compounds	Molecular Weight ^a	pKa ^a	Km (μM)
Bufuralol	261.36	9	3.4 ^b
Debrisoquine	175.23	13.01	73.7 ^c
Imipramine	280.41	9.5	2.68
Desipramine	266.39	10	1.26
Nortriptyline	263.38	9.73	2.08 ^d
Amitriptyline	263.38	9.4	1.61
Propranolol	259.35	9.5	1.48
Dextromethorphan	271.4	8.3	0.58
Metoprolol	267.4	9.68	21.6 ^e
Propafenone	341	9.48	0.01
Spirosulfonamide	387.4	Not positively charged at neutral pH	7.2 ^f
Pactimibe	416.6		25.1 ^g
R-125528	414.6		1.74

^a Molecular weight and pKa for bufuralol, debrisoquine, imipramine, desipramine, nortriptyline, amitriptyline, propranolol,

dextromethorphan, metoprolol, and propafenone are cited from Lewis DFV (2004).

^b Emoto *et al.*, (2006)

^c Shen *et al.*, (2007)

^d Venkatakrishnan *et al.*, (1999)

^e Uttamsingh *et al.*, (2005)

^f Guengerich *et al.*, (2002)

DMD#20776

g Kotsuma *et al.*, (2008)

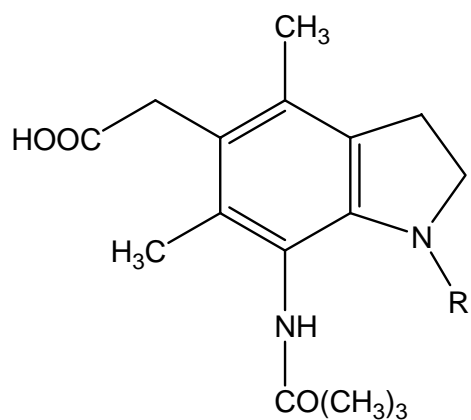
For the determination of the K_m values for imipramine, desipramine, amitriptyline, propranolol, dextromethorphan, and propafenone, the substrate depletion method (Obach and Reed-Hagen, 2002) was used. The final CYP2D6 protein concentration, substrate concentrations, and incubation times were set at 10 pmol/mL, 0.1, 0.3, 1, 3, 10, and 30 μ M, and 0, 3, 6, and 9 min, respectively. The data from the 30 μ M propafenone incubation was excluded from the analysis because log-linear substrate depletion was not clearly observed.

For the determination of the K_m value of R-125528, the formation of M-2 (ω -1 oxidized form of R-125528) up to 15 min was determined. The final CYP2D6 protein concentration and substrate concentrations were set at 10 pmol/mL and 0.3, 1, 3, 10, 30 and 100 μ M, respectively.

DMD#20776

Table 2. Structural analogues of pactimibe and their metabolic stability in CYP2D6

expressing microsomes



Compounds	-R	CYP2D6 Stability (% of 0 min)
Pactimibe	-C ₈ H ₁₇	27.5
R-125528 (indole ring)	-C ₈ H ₁₇	0.8
KV-2908	-C ₆ H ₁₃	97.0
KV-2909	-C ₁₀ H ₂₁	38.1
KV-2915	-C ₁₂ H ₂₅	98.4

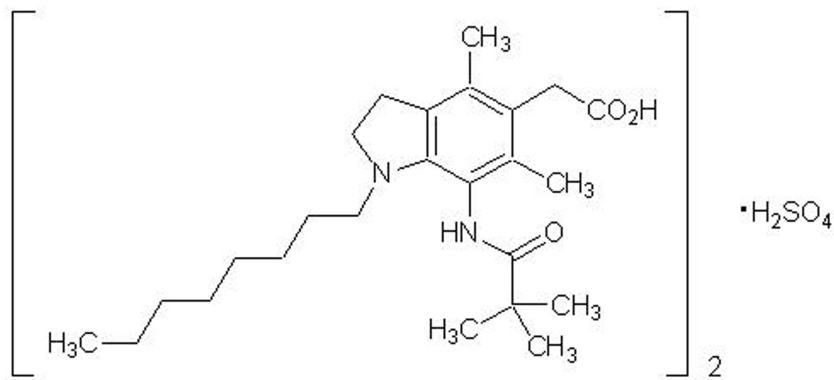
Microsomal incubations were carried out at 37°C for up to 30 min. The final concentrations of CYP2D6 protein and

substrates were set at 40 pmol/mL and 1 μM, respectively. The CYP2D6 stability of each compound is represented as the

remaining percentage at 30 min compared to that at 0 min. Incubations were performed in duplicate.

Figure 1

(A)



(B)

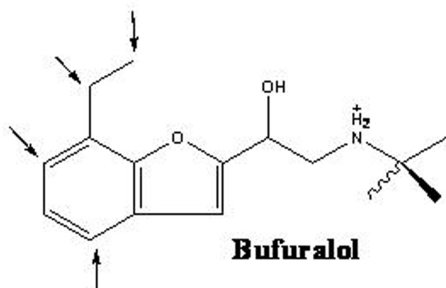
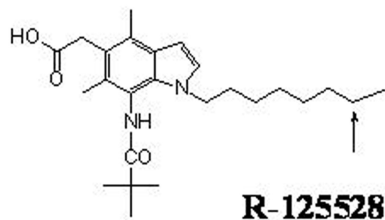
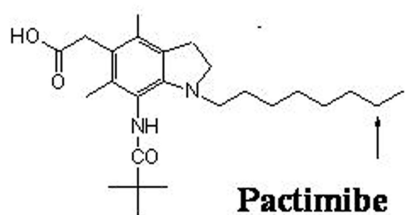
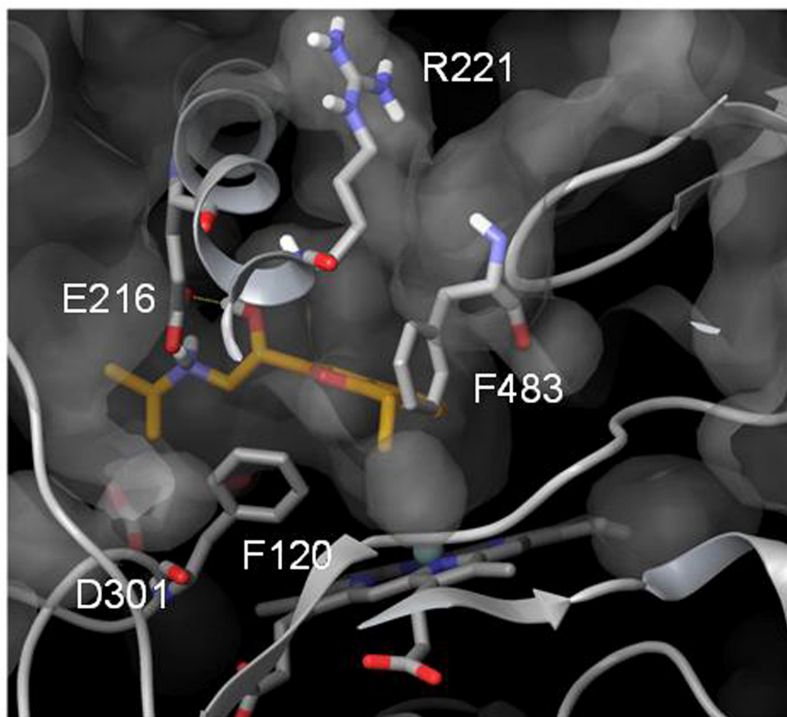


Figure 2

(A)



(B)

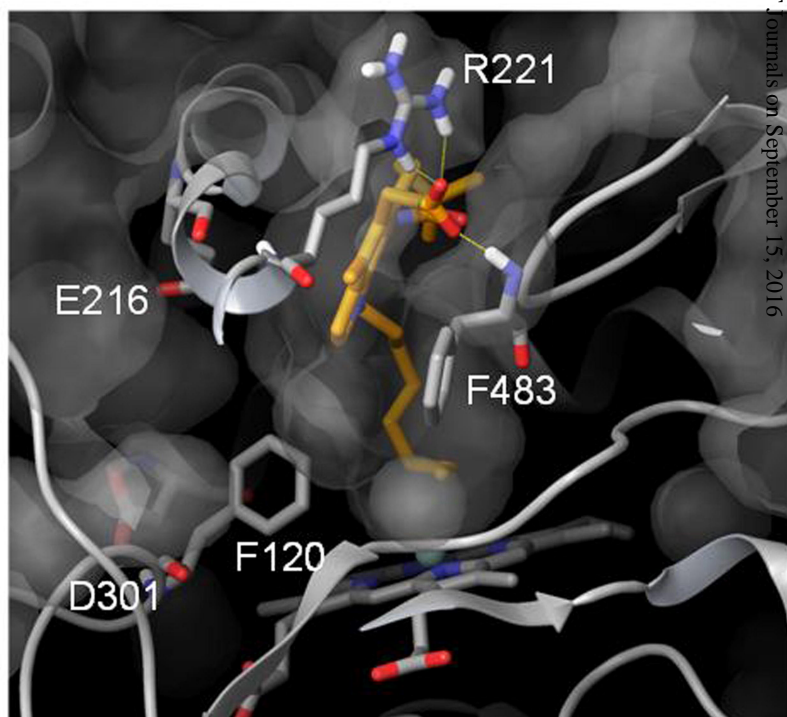


Figure 3

